Journal of Applied Fluid Mechanics, Vol. 9, No. 2, pp. 643-651, 2016.
Available online at www.jafmonline.net, ISSN 1735-3572, EISSN 1735-3645.
DOI: 10.18869/acadpub.jafm.68.225.24407

Numerical Investigation of Non-Stationary Parameters on Effective Phenomena of a Pitching Airfoil at Low Reynolds Number

A. Naderi, M. Mojtahedpoor† and A. Beiki

Aerospace Research Institute, Malek -Ashtar University of Technology, Tehran, Iran

†*Corresponding Author Email: Mojtahedpoor@gmail.com*

(Received December 23, 2014; accepted May 13, 2015)

ABSTRACT

Various applications of ornithopter have led to research interest in oscillation airfoils which affect on low Reynolds number flight, like; pitching oscillation, heaving oscillation and flapping of a wing. The purpose of this study is investigation of aerodynamic characteristics of NACA0012 airfoil with a simple harmonic pitching oscillation at zero and 10 degrees of mean angle of attack. Therefore the effects of unstable parameters, including oscillation amplitude up to 10 degrees, reduced frequency up to 1.0, center of oscillation up to 6/8 chord length, and Reynolds number up to 5000 have been studied numerically. A pressure based algorithm using a finite volume element method has been used to solve Navier-Stokes equations. According to results, variation of each studied parameters at mean angle of attack of 0 degree do not cause significant changes in flow phenomena on airfoil but at mean angle of attack of 10 degrees, changing in reduced frequency and specially Reynolds number cause variations in flow phenomena. These variations are because of "wake capturing" and/or "added mass" phenomena.

Keywords: Oscillation amplitude; Reduced frequency; Center of oscillation; Pitching oscillation.

1. INTRODUCTION

Appearances of flapping MAVs are the main reason for studying of low Reynolds fluid dynamics. These devices are designed in terms of non-stationary flow with moving wings. Due to small size and low speed of free-flow, the range of Reynolds number is too low. The successful design and modeling require the exact solution of the flow field which this solution totally relies on the knowledge of flow pattern and structure. Studies of two-dimensional unsteady low Reynolds number flow is quite useful in perception the flow characteristics and it can be useful in prediction of aerodynamic efficiency dependence on various parameters such as oscillation amplitude, reduced frequency, Reynolds number, and kinematic pattern. Also it reviews major impact on the comprehension of three-dimensional phenomena such as wing vortices, flow in transverse direction and vortex interactions.

Many researchers have been studied low Reynolds number flow around oscillating airfoils numerically, analytically and experimentally. The applications of analytical solution are limited to simplified flows such as quasi-steady solutions or Theodorsen method for two-dimensional oscillation airfoils (Leishman 2006). For a pitching airfoil, which is considered as a representative instance of a non-stationary flow, the most important components are oscillating amplitude, mean angle of attack, reduced frequency and Reynolds number (Chang and Eun 2003). Dynamic stall is generally discussed by researchers because wing motion amplitude is very great over the stall angle. Beyond the stall angle, oscillating amplitude and mean angle of attack are the dominant parameters because they affect leading-edge vortex and trailing-edge vortex formations, which specify aerodynamic performance in dynamic stall (Ohmi *et al.* 1991). However, acceleration effect critically influences boundary-layer events within the stall angle, and it is dominantly dependent on pitching direction (Ericsson and Reding 1988). Kim measured aerodynamic coefficients for a pitching airfoil at $\mathrm{Re} = 4.8\times10^4$ withindoors stall angle of $\alpha = \pm6^o$. In accordance with their study, the unsteady pressure coefficient on the airfoil surface dramatically changed with pitching direction (Kim *et al.* 2013). Jung and Park experimentally demonstrated that the vortices of an oscillating airfoil are strongly influenced by reduced frequency (Jung and Park 2005). Experiments by Fuchiwaki and Tanaka on an oscillating airfoil at Reynolds number of 4000 show that vortices and their sizes depend on reduced frequency. On the other side, these structures are independent of airfoil shape and

set up angle (Fuchiwaki and Tanaka 2006). Koochesfahani have been done many researches in low Reynolds number experimentally and showed frequency and oscillation amplitude have significant effect on vortices structure and propellant coefficient of an oscillating airfoil (Koochesfahani 1989). Shih in a similar study carried the interactions of vortex-vortex and their effects on aerodynamic forces (Shih *et al*. 1995). Akbari and Price simulated flow around an oscillating airfoil at Re=10^4 by solving Navier-Stokes equations and reported reduced frequency and Reynolds number have highest and lowest impact on aerodynamic forces respectively (Akbari and Price 2003) Yung and Lai have studied the effects of frequency and oscillations amplitude on flow field around a two-dimensional airfoil. They showed propellant coefficients are more dependent on the multiplied of $k.\alpha$ to α or k singly where k is reduced frequency and α is angle of attack (Yung and Lai 2004). The effect of Reynolds number in range of $2.0\times10^4 < \mathrm{Re} < 5.0\times10^4$ on aerodynamic characteristics of a pitching NACA0012 airfoil have been experimented (Kim and Chang 2014). In their study, reverse flow and near wake were visualized by smoke-wire flow visualization, and lift and pressure drag coefficients were estimated by measuring unsteady pressure through pressure distortion correction. They was used an airfoil sinusoid-pitched at quarter chord, and its mean angle of attack and oscillation amplitude were $\alpha = 0$ degree and 6 degree respectively. The test Reynolds numbers were $\mathrm{Re} = 2.3\times10^4$, 3.3×10^4 and 4.8×10^4 with reduced frequency of $k = 1.0$. In accordance with their study, the reverse flow visualization, the first and second trailing-edge vortices and mushroom structure depending on the Reynolds number. They showed, in lift and pressure drag coefficients, hysteresis loops comparatively varied with the Reynolds number and so the phase angle, at which boundary-layer events occurred, is in inverse proportion to the increase in Reynolds number. This result implies that the increase in Reynolds number promotes the occurrence of boundary-layer events such as laminar separation and transition (Kim and Chang 2014). The investigations on oscillating airfoils show that the aerodynamic coefficients are affected by oscillation function characteristics dramatically (Amiralaei *et al*. 2010).

The aim of this study is investigation of aerodynamic characteristics of NACA0012 with harmonic pitching oscillation at lower Reynolds numbers. Therefore the effects of unstable parameters, including oscillation amplitude, mean angle of attack, reduced frequency, and Reynolds number have been studied by solving the Navier-Stokes equations. The mean angles of attack were chosen equal to zero and 10 degrees, because at mean angle of attack of zero, the airfoil does not meet separation but at mean angle of 10 degrees separation happens. Therefore, changing flow regime is studied in non-separation and separation situations. We have used a pressure based algorithm using a finite volume element method to solve Navier-Stokes equations.

2. GOVERNING EQUATIONS AND NUMERICAL MODELING

The governing equations including the conservation equations of mass and momentum in Eulerian Lagrangian space is written as follows:

$$\frac{d}{dt}\iiint_{\vartheta(t)} \rho d\vartheta + \iint_{\vartheta(t)} \rho\left(V - V'\right)\cdot dS = 0 \tag{1}$$

$$\frac{d}{dt}\iiint_{\vartheta(t)} \rho V d\vartheta + \iint_{S(t)} \rho V\left(V - V'\right)\cdot dS = \iint_{S(t)} \sigma\hat{n}\cdot dS \tag{2}$$

where $V = u\hat{i} + v\hat{j}$ is flow velocity vector, $V = u'\hat{i} + v'\hat{j}$ is control volume surfaces velocity vector, $dS = (dS_{\mathbf{x}})\hat{\mathrm{i}} + (dS_{\mathbf{y}})\hat{\mathrm{j}}$ is normal vector to surface with magnitude of $dS = \left[(dS_{\mathbf{x}})^2 + (dS_{\mathbf{y}})^2\right]^{1/2}$, $\hat{\boldsymbol{n}} = (n_{\mathbf{x}})\hat{\boldsymbol{i}} + (n_{\mathbf{y}})\hat{\boldsymbol{j}}$ is a unit normal vector to surface and ϑ is volume which is related to control volume. σ is total stress tensor which includes hydrostatic pressure p, and shear stress tensor $\sigma_{ij} = -p\delta_{ij} + \tau_{\mathrm{ij}}$.

Geometric conservation equation is in mass conservation equation. If the fluid particle velocity is zero and density of the fluid is one, the mass conservation equation for each swept surface of control volume will calculated by:

$$V'\cdot dS\big|_m = \left.\frac{d\mathcal{V}}{dt}\right|_m \tag{3}$$

where m is surfaces counter of each finite volume and $\mathcal{V}$ is related volume to each finite sub-volume. Figure 1 shows a control volume which includes 5 sub control volumes (SCV) and the surround consist of 10 surfaces (SS).

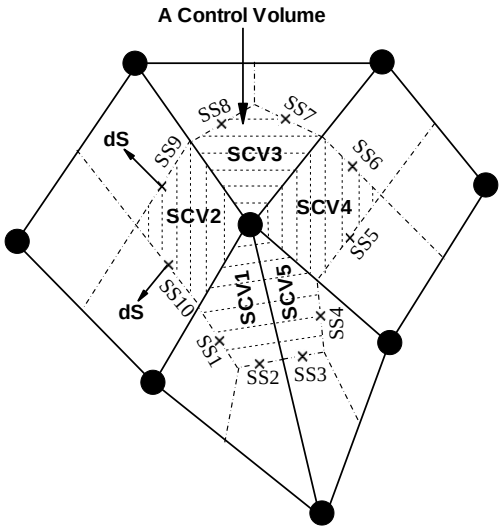

Fig. 1. A control volume consist of 5 SCV and 10 SS.

If Eq. (3) always satisfied, the volume conservation of SCV will be established. In other words, the swept surface of SCV shall be calculated that by using of Eq. (3), the exact amount of $d\mathcal{V}/dt$ is reached. We have used the second-order approach to approximate SCV derivation:

$$\frac{d\mathcal{V}}{d\mathrm{t}} \cong \frac{(3/2)\mathcal{V}^{n+1} - 2\mathcal{V}^{n} + (1/2)\mathcal{V}^{n-1}}{\Delta \mathrm{t}} \tag{4}$$

where n is counts time steps. By performing a series of arithmetic operations on the above equation it can be rewritten as follows:

$$\frac{d\mathcal{V}}{dt} \cong \frac{(3/2)(\Delta\mathcal{V}^{n+1}) - (1/2)(\Delta\mathcal{V}^{n})}{\Delta t} \tag{5}$$

where $\Delta\mathcal{V}^{n+1} = \mathcal{V}^{n+1} - \mathcal{V}^{n}$ and $\Delta\mathcal{V}^{n} = \mathcal{V}^{n} - \mathcal{V}^{n-1}$.

If movement of surface causes increasing in volume SCV the amount of $\Omega = d\vartheta/dt$ become positive and vice versa. By using of this relation, one part of momentum equation which includes the coefficient of grid movement effects can be rewritten for each swept surface as follow

$$V(V') \cdot dS\big|_{m} = V\Omega\big|_{m} \tag{6}$$

Coupling of mass and momentum equations, and also, approximation of convection, diffusion and pressure terms performs by a finite volume element method in Eulerian Lagrangian space such as in Eulerian space (Naderi *et al.* 2009).

3. CASE AND PREPROCESSING STUDIES

To investigate the effects of non-stationary parameters of pitching airfoil we have considered NACA0012 airfoil at meant angle of attack of zero and 10 degrees. The chord length, "c" is unit and other lengths are nondimensionalized with it. NACA 0012 airfoil oscillating function is $\alpha(t) = \alpha_0 + \alpha_1 \sin(2\pi f \times t)$, where α_0 is mean angle of attack, α_1 is oscillation amplitude and f is frequency which is nondimensionalized with reduced frequency, k as $k = \pi fc/U_\infty$. Free stream velocity is U_∞ which has a unit magnitude and other velocities are nondimensionalized with it.
The effects of oscillation amplitude, reduced frequency, Reynolds number and center of oscillation location on aerodynamic coefficients have been investigated. For these simulations the defaults amounts have been set in table 1 and case characterization has been illustrated in Fig. 2.

We have used unstructured grid for this study. Figure 3 shows some part of the grid before pitching movement. Also we have considered tetrahedral grid on airfoil and the unstructured triangular gird up to free boundaries, inlet and outlet. Our strategy of using hybrid grids on internal and external flow was described exactly in reference (Darbandi and Naderi 2006). The distance of center of airfoil from free boundaries and outlet is 30. The outlet pressure is also unit, length scale and velocity scale in Reynolds number and reduced frequency formulations are chord length and free stream velocity, respectively. Also, time is nondimensionalized with them.

Table 1 Case studies

Variables	Reduced frequency	Oscillation amplitude	Reynolds number	x/c Ratio
Oscillation amplitude	0.5	2^0~10^0	1000	1/4
Reduced frequency	0.125 ~ 1	10^0 and 5^0	1000	1/4
Reynolds number	0.5	10^0 and 5^0	1000 ~5000	1/4
x/c Ratio	0.5	10^0 and 5^0	1000`	1/8~6/8

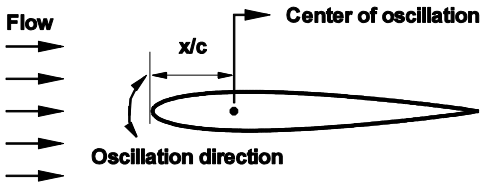

Fig. 2. Case characterization.

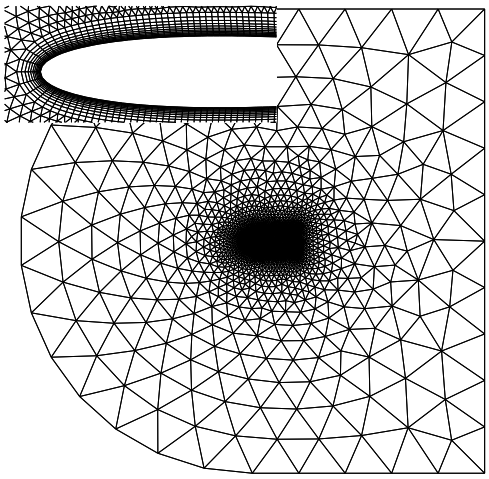

Fig. 3. Unstructured gird around the airfoil.

To investigate the sensitivity of solution to computing grid, three grids with different node number of 5989, 8130 and 10547 have been used. Figure 4 shows the sensitivity of solution to the grids in Reynolds number of 5000. In accordance with Fig. 4, we can use the grid with number of 8130 nodes in the next computations. Similarly, to determine the sensitivity of the solution to the time steps, we have solved the flow in time steps of 0.025, 0.05 and 0.1 in Reynolds number of 5000 separately. The obtained results have been illustrated in Fig. 5. According to Fig. 5, the time step in all other computations has been set to 0.05.

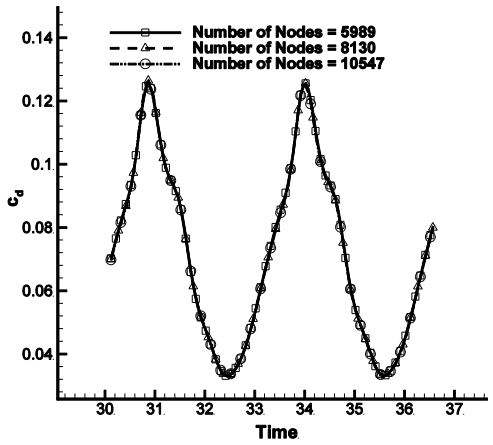

Fig. 4. Investigation of grid-independency in Reynolds number of 5000, drag coefficient.

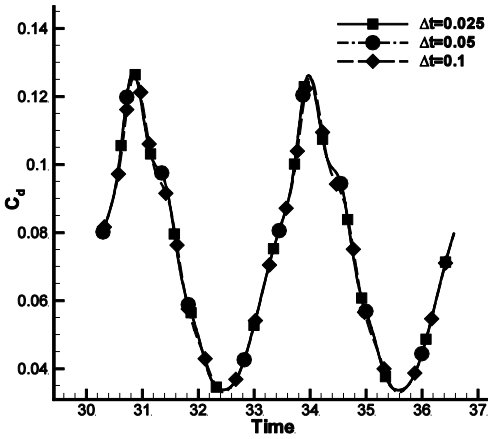

Fig. 5. Investigation of time-step-independency in Reynolds number of 5000, drag coefficient.

To further validate our written code, the pure pitching sinusoidal motion of a NACA0012 airfoil with amplitude of 5º and reduced frequency of 9 at $Re=1.35\times10^4$ was simulated. The comparison of lift coefficient between our computational results and Lu (K. Lu *et al.* 2013) is shown in Fig. 6.

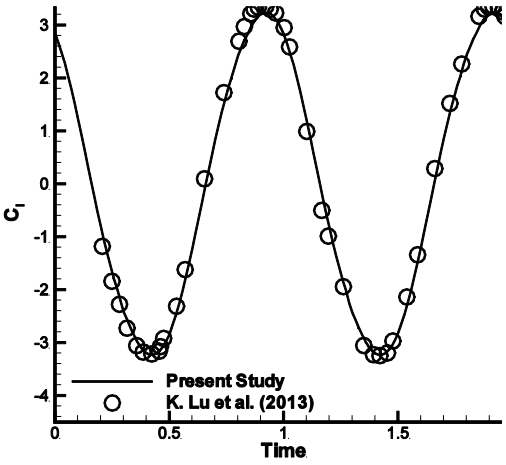

Fig. 6. Variation of lift coefficient with time at reduced frequency of 9 and amplitude of 5º for a pitching NACA0012 airfoil (Re=13500).

As can be seen, our numerical predictions agree with the computational results by other researcher very well.

4. RESULTS

4.1 Effects of Oscillation Amplitude

Effects of oscillation amplitude on aerodynamic coefficients in Reynolds number of 1000 and reduced frequency of 0.5 have been illustrated in Figs. 7 and 8. In accordance with Fig. 7, the maximum lift is more at higher oscillation amplitudes. Also the width of lift curve became greater for higher amplitudes. The lift production at higher oscillation amplitude at upstroke– in a same angle of attack than stationary airfoil- is more and also at downstroke is less than stationary airfoil. Lift coefficient in upstroke is more than downstroke. Figure 8 shows maximum of drag increase and its minimum decrease. A minimum and maximum amount of drag coefficients will be appeared in upstroke and downstroke that the maximum amounts are equal and minimums are equal also. The drag coefficient at zero angle of attack is not almost influenced by oscillation amplitude.

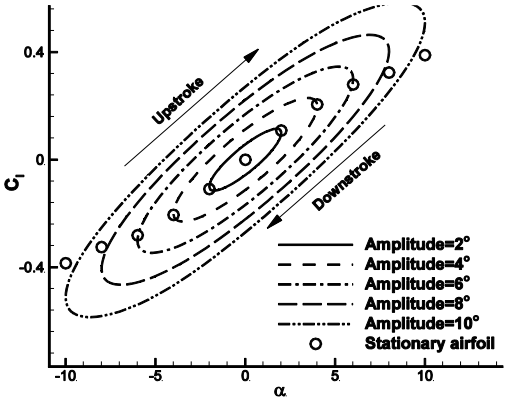

Fig. 7. Effects of oscillation amplitude on lift coefficient at mean angle of attack of 0 degree (Re=1000).

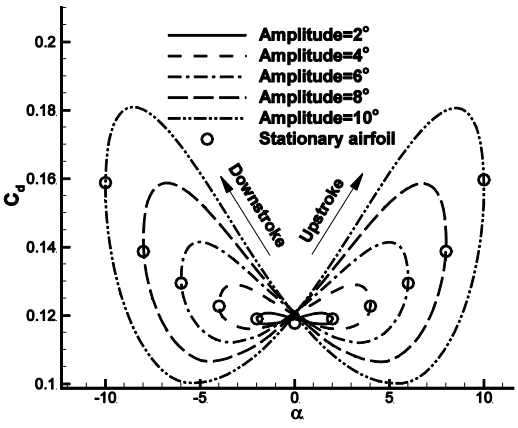

Fig. 8. Effects of oscillation amplitude on drag coefficient at mean angle of attack of 0 degree (Re=1000).

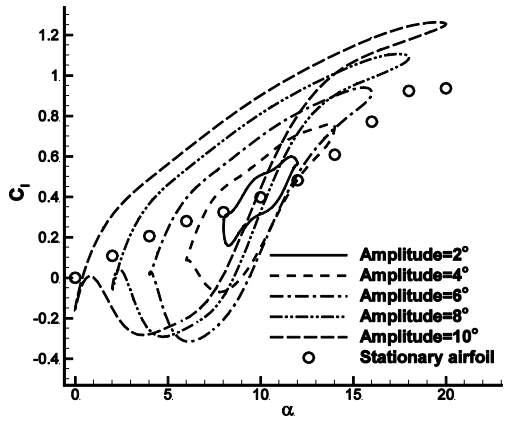

Fig. 9. Effects of oscillation amplitude on lift coefficient at mean angle of attack of 10degree (Re=1000).Copyright.

Figures 9 and 10 show, effects of oscillation amplitude on lift and drag coefficients at mean angle of attack of 10 degrees. In accordance with Figs. 9 and 10, by increasing of oscillation amplitude, minimum amounts of lift and drag a little varied at higher amplitudes but the maximum amounts increased gradually. Lift and drag coefficients curves treat as expected by increasing amplitude.

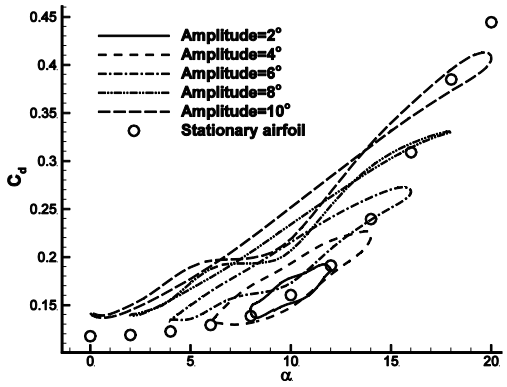

Fig. 10. Effects of oscillation amplitude on drag coefficient at mean angle of attack of 10degree (Re=1000).

4.2 Effects of Reduced Frequency

Effects of reduced frequency on the aerodynamic coefficients in oscillation amplitude of 10 degrees, mean angle of attack of 0 degree and Reynolds number of 1000 have been shown in Figs. 11 and 12.

According to Fig. 11, the width of oscillation curve increases by growth of reduced frequency, indeed, in reduced frequency of 1.0 the growth in oscillation curve width is more than other frequencies. According to Fig. 12, maximum of drag coefficient increases, and minimum drag coefficient decreases and oscillation curve width has increased by increasing of reduced frequency.

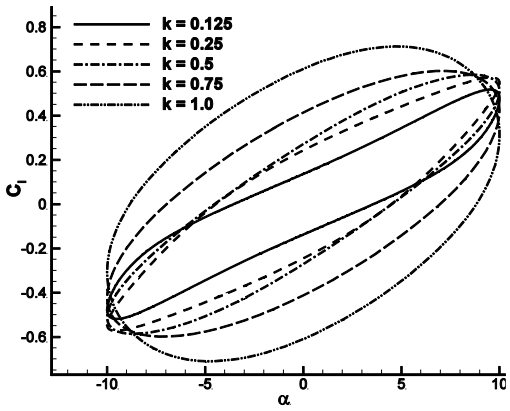

Fig. 11. Effects of reduced frequency on lift coefficient at mean angle of attack of 0 degree (Re=1000).

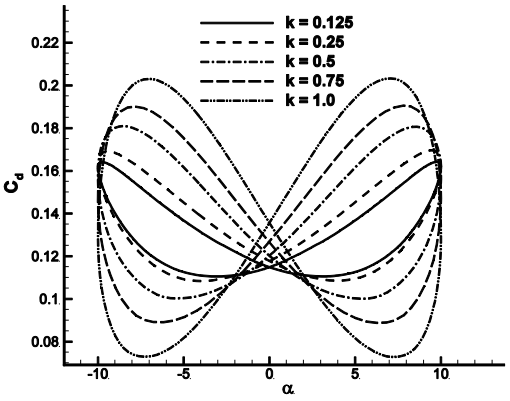

Fig. 12. Effects of reduced frequency on drag coefficient at mean angle of attack of 0 degree (Re=1000).

At $k = 1$, the minimum and maximum amounts of drag coefficient in upstroke and downstroke are happened at about $\alpha \sim \pm 8$ degree. Also, the drag coefficient at zero angle of attack has increased by increasing of reduced frequency. By increasing of k significant changes has not been seen in behavior of coefficients curves.

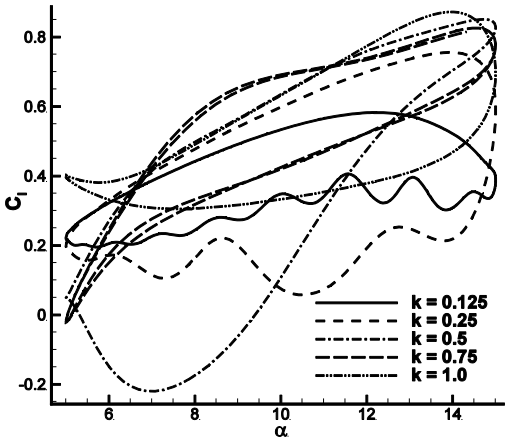

Fig. 13. Effects of reduced frequency on lift coefficient at mean angle of attack of 10 degree (Re=1000).

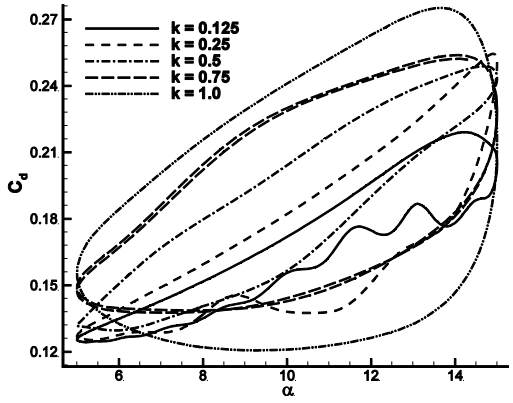

Fig. 14. Effects of reduced frequency on drag coefficient at mean angle of attack of 10 degrees (Re=1000).

Figures 13 and 14 show, effects of reduced frequency at mean angle of attack of 10 degrees. Accordance with these figures, by increasing of reduced frequency, the behavior of the curves are changing and this means some different phenomena affect on airfoil by increasing reduced frequency. According to (Andro and Jacquin 2009) at low frequencies, aerodynamic forces result from the quasi-steady plus leading edge vortex and by increasing of frequency, they are results from wake-capture and added mass phenomena.

4.3 Effects of Reynolds Number

Effects of Reynolds number on the aerodynamic coefficients in reduced frequency of 0.5 and oscillation amplitude of 10 degrees have been shown in Figs. 15 and 16. Lift coefficients change a little with increasing Reynolds number up to Re=5000 where it seems the flow effects is changed. The drag coefficient is decreased dramatically by increasing of Reynolds number. Lift and drag coefficients are predictable at each Reynolds number, except at Re=5000.

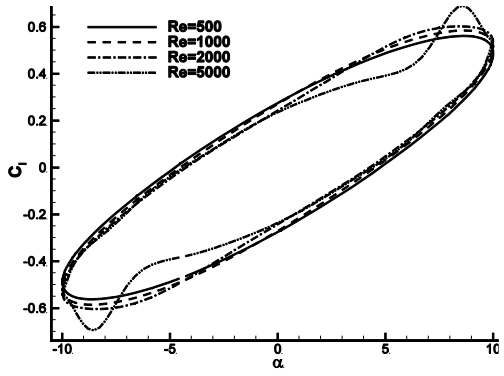

Fig. 15. Effects of Reynolds number on lift coefficient at mean angle of attack of 0 degree.

Streamlines comparisons at Re=500 and Re=5000 at the situation that the airfoil is oscillating with mean angle of attack of zero degree and it is located at its maximum angle of attack have been illustrated in Figs. 17.a and 17.b, respectively.

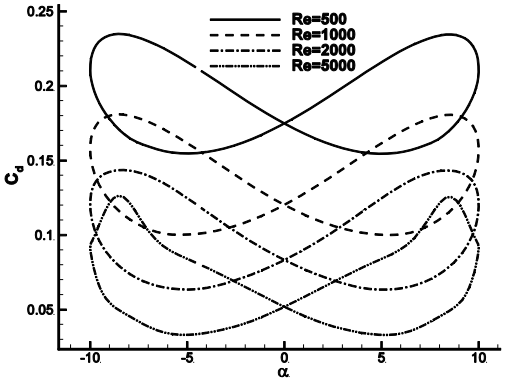

Fig. 16. Effects of Reynolds number on drag coefficient at mean angle of attack of 0 degree.

In accordance with Fig 17.a and 17.b, there are two light separation at the trailing edge. However at Re=5000, a fluctuation wave is produced in the wake region. This fluctuation comes from a vortex generation and breakdown at the trailing edge. This phenomena affects on lift and drag coefficients where the airfoil is located on its maximum and minimum positions.

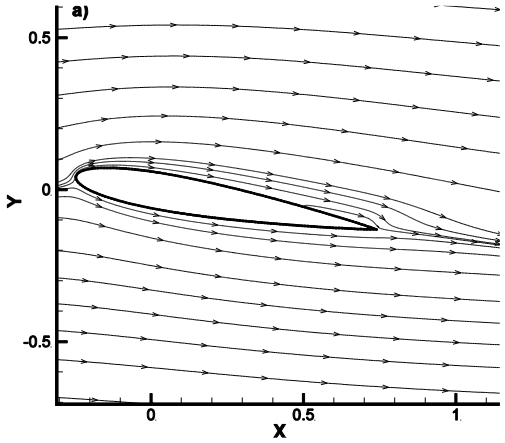

Fig. 17.a. Streamlines at Re=500; α= 10 degrees.

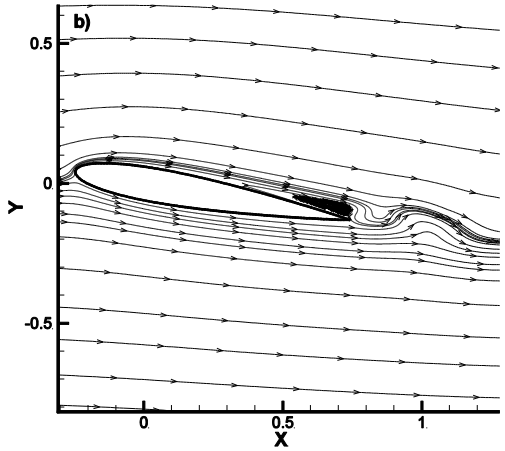

Fig. 17.b. Streamlines at Re=5000; α= 10 degrees.

Effects of Reynolds number on lift and drag coefficients at mean angle of attack of 10 degrees have been shown in Figs. 18 and 19. According to Fig. 18, by increasing of Reynolds number from

500 to 1000, 2000 and 5000 some complexity will be appeared. This complexity causes that the periodic effect of c_l and c_d was occurred through two stroke of oscillation at Re=5000 while in other Reynolds numbers the periodic effects were occurred through one stroke.

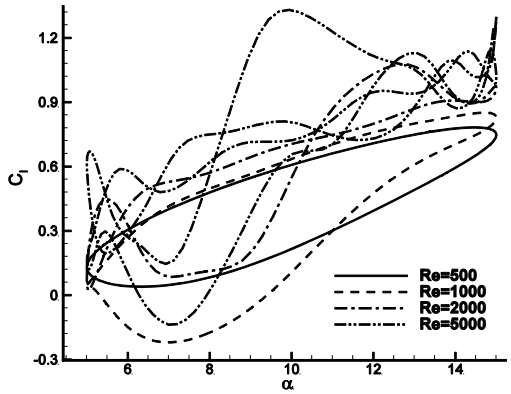

Fig. 18. Effects of Reynolds number on lift coefficient at mean angle of attack of 10 degree.

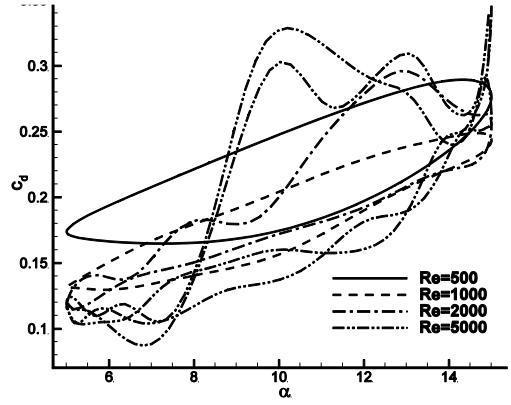

Fig. 19. Effects of Reynolds number on drag coefficient at mean angle of attack of 10 degree.

For instance, we have used FFT (Fast Fourier Transform) graph of c_l to show dominant frequency and other frequencies, at different Reynolds number. According to Fig. 20, by increasing of Reynolds number, the numbers of picks have increased gradually, but in all Reynolds number the dominant frequency is about 0.15 which is oscillation frequency of pitching airfoil.

Also Fig. 21 shows, wall friction and pressure coefficient on airfoil at different Reynolds number where airfoil is located at its maximum angle of attack. As it is obvious from Fig. 21, c_f and c_p are changed smoothly at Re=500, 1000, 2000 while at Re=5000 some deviations are appeared.

Andro analyzed the three fundamental mechanisms that govern aerodynamic efforts acting on pitching airfoil which two important of them at high angle of attack and high frequencies are "added mass" reaction and "wake capture" (Andro and Jacquin 2009). Added mass force explains the mass of fluid displaced with the airfoil and it is maximum when acceleration reaches its maximum. This force is proportional to $A_0\omega^2$ and varies linearly as the square of frequency which A_0 is amplitude and ω is angular frequency (Andro and Jacquin 2009). Also Birch and Dickinson expressed when vortex captured on the rear side of airfoil, the unsteady mechanism which called "wake capture" will be happened (Birch and Dickinson 2003). This force strongly depends on both kinematics and frequency. Reynolds number is the main scaling parameters here, because it fixes the maximum aerodynamic incidence which itself strongly determines the strength of leading edge vortex. From Figs. 18 and 19, at Re=5000, the main peak of c_l and c_d is occurred at $\alpha \approx 10$ degree, the beginning of the stroke when acceleration reaches its maximum value. The secondary peak is occurred at $\alpha \approx 15$ degree, the end of stroke when wake sticks severely rear at a part of airfoil. In accordance with mean angle of attack of 10 degrees, Reynolds number of 5000, c_p and c_f graphs, it seems the complexity in Figs. 18 and 19 is because of wake capture and/or added mass forces.

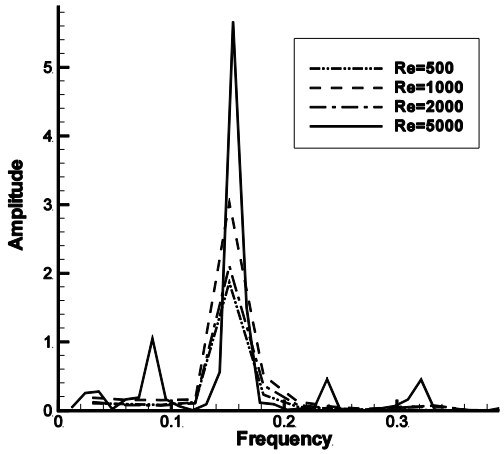

Fig. 20. FFT graph at Reynolds number of 5000 and mean angle of attack of 10.

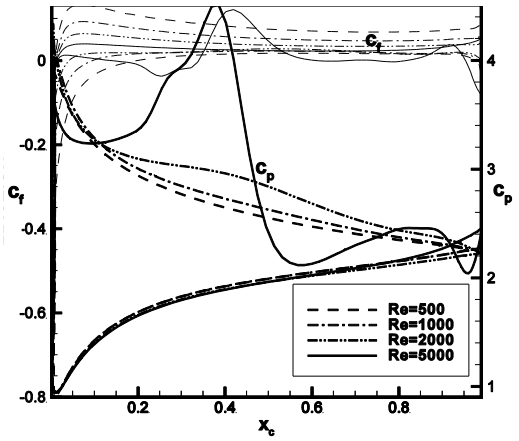

Fig. 21. Wall friction and pressure coefficient graph at different Reynolds number and mean angle of attack of 10 degrees.

4.4 Effects of Center of Oscillation

Effects of x/c ratio, the center of oscillation have been investigated in this part. Figure 22 shows the

effects of center of oscillation on lift coefficient.

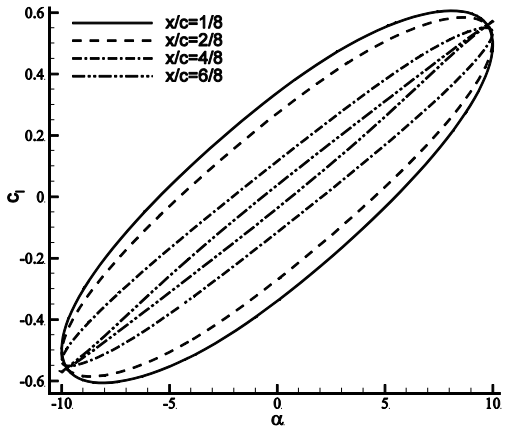

Fig. 22. Effects of center of oscillation on lift coefficient (Re=1000).

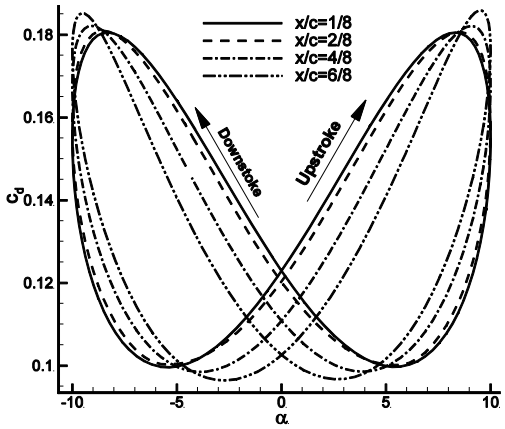

Fig. 23. Effects of x/c ratio on drag coefficient (Re=1000).

In accordance with Fig. 22, by increasing of x/c ratio from 1/8 to 6/8, width of lift coefficient curve decreases and its minimum and maximum do not change significantly. According to Fig. 23, the width of drag coefficient curve decreases when x/c increases. There is no significant change in the maximum and minimum amounts also. Drag coefficient has decreased at angle of attack of 0 degree, by increasing of x/c ratio. The behaviors of the curves do not change with x/c ratio changing and they are predictable.

5. CONCLUSION

The purpose of this study is investigation of aerodynamic characteristics of NACA0012 with harmonic pitching oscillation at zero and 10 degrees mean angles of attack. Therefore the effects of unstable parameters, including oscillation amplitude, reduced frequency, Reynolds number and center of oscillation have been studied. A pressure based algorithm using a finite volume element method to solve Navier-Stokes equations has been used.

Results show, by increasing of oscillation amplitude at mean angle of attack of 0 degree, the width of lift coefficient curve has increased gradually. Also by increasing of oscillation amplitude the minimum and maximum amount of drag and lift coefficients have increased sharply. Also, this behavior has been seen at mean angle of attack of 10 degrees and lift and drag coefficients curves have varied as expected.

By increasing of reduced frequency, the maximum values of lift and drag coefficients have increased, their minimums have decreased and the width of oscillation curves increased. Also, the drag coefficient at zero angle of attack has increased by increasing of reduced frequency. By changing of reduced frequency at mean angle of attack of 10 degrees, the behaviors of the curves have been varied. This variation is because of wake capture and added mass phenomena.

By increasing of Reynolds number at mean angle of 0 degree, significant changes have not seen in lift curves except at Reynolds number of 5000 where it seems the flow regime is changed, but the maximum and minimum amounts of drag coefficients at zero angle of attack have decreased acutely. At mean angle of attack of 10 degrees, dominant frequency in different Reynolds numbers was observed 0.15 Hz which is oscillation frequency. At Reynolds number of 5000 and at high angle of attacks, some complexity will be appeared in lift and drag coefficients because wake capturing and/or added mass phenomena which are dominant effects.

By increasing of center of oscillation up to 6/8 chord length (x/c ratio), lift coefficient curve has decreased and its minimum and maximum have not changed excessively. Drag coefficient has decreased at angle of attack of 0 degree, by increasing of x/c ratio. The manners of the curves do not change with x/c ratio changing and they varied as expected.

REFERENCES

Akbari, M. H. and S. J. Price (2003). Simulation of dynamic stall for a NACA0012 airfoil using a vortex method. *Journal of Fluid and Structures* 17(6), 855-874.

Amiralaei, M. R., H. Alighanbari and S. M. Hashemi (2010). An investigation into the effects of unsteady parameters on the aerodynamics of a low Reynolds number pitching airfoil. *Journal of Fluid and Structures* 26(6), 979-993.

Andro, J. Y. and L. Jacquin (2000). Frequency effects on the aerodynamic mechanisms of a heaving airfoil in a forward flight configuration. *Aerospace Science and Technology* 13(1), 71-80.

Birch, J. M. and M. H. Dickinson (2003). The influence of wing-wake interactions on the production of aerodynamic forces on production of in flapping flight. *Journal of experimental biology* 206, 2257-2272.

Chang, J. W. and H. B. Eun (2003). Reduced frequency effects on the near-wake of an oscillating elliptic airfoil. *KSME International Journal* 17(8), 1234-1245.

Darbandi, M. and A. Naderi (2006). Multiblock hybrid grid finite volume method to solve flow in irregular geometries. *Computer Methods in Applied Mechanics and Engineering* 196(1), 321-336.

Ericsson, L. E. and J. P. Reding (1998). Fluid mechanics of dynamics stall. Part1. Unsteady flow concepts. *Journal of Fluid and Structures* 2, 1-33.

Fuchiwaki, M. and K. Tanaka (2006). Vortex structure and scale on an unsteady airfoil. *JSME International Journal* 49, 1056-1063.

Jung, Y. W. and S. O. Park (2005). Vortex-shedding characteristics in the wake of an oscillating airfoil at low Reynolds number. *Journal of Fluid and Structures* 20(3), 451-464.

Kim, D. H. and J. W. Chang (2014). Low-Reynolds-number effect on the aerodynamic characteristics of a pitching NACA0012 airfoil. *Aerospace Science and Technology* 32, 162-168.

Kim, D. H., J. W. Chang and H. B. Kim (2013). Aerodynamic characteristics of a pitching airfoil through pressure distortion correction in pneumatic tubing. *Journal of Aircraft* 50(2), 590-598.

Koochesfahani, M. M. (1989). Vertical patterns in the wake of an oscillating airfoil. *AIAA Journal* 27, 1200-1205.

Leishman, J. G. (2006). Principles Aerodynamics, 2nd Edition. *Cambridge University Press*, London.

Lu, K., Y. H. Xie and D. Zhang (2013). Numerical study of large amplitude, nonsinusoidal motion and chamber effects on pitching airfoil propulsion, *Journal of Fluids and Structures* 35, 184-194.

Naderi, A., M. Darbandi and M. Taeibi-Rahni (2009). Developing a unified FVE-ALE approach to solve unsteady fluid flow with moving boundaries. *International Journal of Numerical Method in Fluids* 63(10), 40-68.

Ohmi, K., M. Coutanceau, O. Daube and T. P. Loc (1991). Further experiments on vortex formation around an oscillating and translating airfoil at large incidences. *Journal of Fluid Mechanics* 255, 607-630.

Shih, C., L. M. Lourenco and A. Krothapalli (1995). Investigation of flow at leading edges of pitching-up airfoil. *AIAA Journal* 33, 1369-1376.